

IMPROVED PHOTOMETRIC CALIBRATIONS FOR RED STARS OBSERVED WITH THE SDSS PHOTOMETRIC TELESCOPE

JAMES R. A. DAVENPORT^{1,2}, JOHN J. BOCHANSKI², KEVIN R. COVEY³, SUZANNE L. HAWLEY², ANDREW A. WEST⁴,
DONALD P. SCHNEIDER⁵

Accepted for publication in AJ

ABSTRACT

We present a new set of photometric transformations for red stars observed with the Sloan Digital Sky Survey (SDSS) 0.5-m Photometric Telescope (PT) and the SDSS 2.5-m telescope at the Apache Point Observatory in New Mexico. Nightly PT observations of US Naval Observatory standards are used to determine extinction corrections and calibration terms for SDSS 2.5-m photometry. Systematic differences between the PT and native SDSS 2.5-m *ugriz* photometry require conversions between the two systems which have previously been undefined for the reddest stars. By matching $\sim 43,000$ stars observed with both the PT and SDSS 2.5-m, we extend the present relations to include low-mass stars with colors $0.6 \leq r - i \leq 1.7$. These corrections will allow us to place photometry of bright, low-mass trigonometric parallax stars previously observed with the PT on the 2.5-m system. We present new transformation equations and discuss applications of these data to future low-mass star studies using the SDSS.

Subject headings: stars: low-mass, brown dwarfs — stars: late-type – surveys: calibration, SDSS

1. INTRODUCTION

The study of low-mass stars has blossomed with the advent of large scale surveys. Due to their low intrinsic luminosity ($\lesssim 10^{-2}L_{\odot}$) and the small fraction of light emitted in the optical band, most prior large area surveys have been limited to nearby objects. Recent surveys such as the Sloan Digital Sky Survey (SDSS; York et al. 2000) and the Two Micron All-Sky Survey (2MASS; Skrutskie et al. 1997) have now produced extensive volumes of photometry and spectroscopy on cool stars (eg. Strauss et al. 1999; Hawley et al. 2002; Walkowicz et al. 2004; West et al. 2004, 2005, 2006; Bochanski et al. 2007a; Covey et al. 2007). Studying these faint neighbors gives us insight into the most numerous stellar population in the Galaxy, probing both young and old subsets of low-mass stars, and placing their properties, such as abundances and dynamics, in a Galactic context (Hawley et al. 2002; Chiu et al. 2006; Metchev et al. 2007). Ongoing studies seek to measure the luminosity function and mass function of low-mass stars (Covey et al. 2007), the dynamics of the thin and thick disks of the Milky Way (Bochanski et al. 2007b), and to characterize magnetic activity and dynamical heating in the Galactic disk (West et al. 2004, 2006, 2007).

These studies are enabled by SDSS photometry due to its high sensitivity, near-infrared bandpasses, and accurate photometry which achieves a relative precision of 2-3% (Ivezić et al. 2004). However, creating a suitable calibration onto an absolute system for SDSS photometry over the entire range of stellar colors poses a great challenge. US Naval Observatory (USNO) measurements of 158 standard stars form the foundation for the SDSS photometric calibration (Fukugita et al. 1996; Smith et al. 2002). These standards are observed on the $u'g'r'i'z'$ system and are comprised mainly of early-type ($<$ spectral class M) stars too bright to be imaged with the SDSS 2.5-m, but which have well defined magnitudes.

The SDSS Photometric Telescope (PT), with an aperture of 0.5-m, is employed to transfer the photometric calibration from the USNO measurements to the SDSS. Located alongside the SDSS 2.5-m telescope (Gunn et al. 2006) at Apache Point Observatory (APO), the PT provides nightly observations on the $u'g'r'i'z'$ photometric system.⁶ By imaging patches of sky coincident with the SDSS nightly footprint, the PT is able to provide a robust calibration between the $u'g'r'i'z'$ and native SDSS 2.5-m *ugriz* systems. Tucker et al. (2006), hereafter T06, details this three telescope calibration method, including the data reduction pipeline (MTPIPE) created for the PT.

Unfortunately, the transformations described in T06 are defined only for limited ranges in color-space. These ranges, listed in Table 1, are too blue for low-mass star studies (Bochanski et al. 2007a; West et al. 2005). In particular, (*ugriz*)_{PT} photometry⁷ diverges from the (*ugriz*)_{SDSS} stellar locus for stars redder than $(r - i)_{SDSS} \geq 0.6$, as shown in Figure 1. These systematic offsets are not unexpected, due to physical differences between the $u'g'r'i'z'$ and *ugriz* filters and the complex calibration between the two native telescope systems (T06). Additional correction terms are

¹ Corresponding author: uwjim@astro.washington.edu

² Department of Astronomy, University of Washington, Box 351580, Seattle, WA 98195

³ Harvard-Smithsonian Center for Astrophysics, 60 Garden Street, MS-72, Cambridge, MA 02138

⁴ Astronomy Department, University of California, 601 Campbell Hall, Berkeley, CA 94720-3411

⁵ Department of Astronomy and Astrophysics, The Pennsylvania State University, 525 Davey lab, University Park, PA, 16802

⁶ The PT telescope uses a $u'g'r'i'z'$ filter set, and the PT data are first calibrated to the USNO $u'g'r'i'z'$ system before being transformed into SDSS *ugriz* magnitudes.

⁷ The expression (*ugriz*)_{PT} denotes PT photometry which has been transformed from the native PT $u'g'r'i'z'$ to the standard SDSS 2.5-m *ugriz* system using the T06 calibrations. We adopt the subscript notation (*ugriz*)_{SDSS} for native SDSS 2.5-m photometry.

needed to rectify this systematic offset, thus placing red stars observed with the PT on the native SDSS 2.5-m system.

An important application of these calibrations would permit PT observations of bright trigonometric parallax stars to be placed on the $(ugriz)_{SDSS}$ system. This will improve distance determinations from photometric parallaxes for low-mass stars, which would greatly benefit many of the studies described above.

In this paper we present analysis of photometry for $\sim 43,000$ red point sources with both SDSS 2.5-m and PT detections. These data are used to derive transformations between the $(ugriz)_{PT}$ and $(ugriz)_{SDSS}$ systems for stars with $0.6 \leq (r-i) \leq 1.7$. Our SDSS and PT sample selection is described in §2. In §3, we present our transformation equations for red stars between the two systems. A discussion of the implications of this improved calibration for low-mass star studies is presented in §4.

2. SAMPLE SELECTION

2.1. SDSS Sample

Our data are taken from the 8000 sq. degrees of the SDSS Data Release 5 (DR5; Adelman-McCarthy et al. 2007). Technical descriptions of the survey can be found in the references in the introduction as well as in Gunn et al. (1998), Hogg et al. (2001), Pier et al. (2003), and Stoughton et al. (2002).

To generate a photometric catalog of low-mass stars in the $(ugriz)_{SDSS}$ system, we queried the Catalog Archive Server⁸ for photometric observations classified as stars with the colors of $r-i > 0.5$ and $i-z > 0.3$ within the DR5 footprint. To ensure accurate point spread function (psf) photometry, several photometric quality flags were imposed on the data.⁹ The final sample contained approximately 13.6 million stars. The brightness distribution of these objects is shown in Figure 2. Because our goal was only to compare the photometric response of red stars between the $ugriz$ and $u'g'r'i'z'$ systems, no corrections for galactic extinction were used.

2.2. PT Sample

During normal photometric operations on the SDSS 2.5-m telescope, the PT automatically images overlapping patches of the sky for calibration. These patches are roughly 15° apart and cover every stripe (great circle path of scan) in the SDSS survey. Typically these images are used to create photometric zero-point ‘anchors’ for the SDSS data onto the USNO system. However, these patches also contain many stars which are not used in the SDSS calibration, but are reduced and saved by MTPIPE (T06). Over five million background star observations were made with the PT during the first six years of SDSS observations. These reduced MTPIPE data are available via the SDSS Data Archive Server.¹⁰

After removing stars which MTPIPE flagged as having bad photometry (magnitude = -100), the PT sample was selected using two color cuts. Low-mass candidates were selected by requiring $(r-i)_{PT} > 0.5$ (Bochanski et al. 2007a). A further color cut of $1.1 \leq (g-r)_{PT} \leq 1.7$ was used to isolate the low-mass stellar locus, removing carbon stars (Fan 1999). This process yielded $\sim 345,000$ stars with red colors which have accurate PT magnitudes. The PT sub-sample has mean magnitude errors of $\sigma(g_{PT}) = 0.05$, $\sigma(r_{PT}) = 0.07$, $\sigma(i_{PT}) = 0.08$, and $\sigma(z_{PT}) = 0.06$. We did not use the u_{PT} data due to the lack of good photometry for these red stars; only $\sim 12,000$ stars in the PT sample have good u_{PT} photometry ($\sigma(u_{PT}) \leq 0.05$).

2.3. Matched Sample

To facilitate matching between the two samples, we imposed a bright magnitude limit on the PT sample to isolate stars potentially observed by both telescopes (See Figure 2). In particular, the following magnitude cuts were used on the PT sample: $15.4 \leq g_{PT} \leq 21.5$; $14.6 \leq r_{PT} \leq 20.0$; $14.0 \leq i_{PT} \leq 19.7$; $14.1 \leq z_{PT} \leq 19.5$.

The PT and SDSS samples were matched by celestial position, yielding 42,912 PT-2.5-m matches within a search radius of $0.5''$. The SDSS 2.5-m astrometry is accurate to $0.045''$, while the PT astrometry is accurate to $\sim 1''$. As we are not trying to find a complete sample, we chose a conservative search radius ($0.5''$) to minimize mismatches, and still obtain a large number of matches. Since typical proper motions of these stars were small over the limited time range of PT observations (2002 – 2007), the loss of some high proper-motion stars was negligible.

3. RESULTS

3.1. Determining Offsets

Using the matched sample described in §2.3, the magnitude differences between the two systems were determined for each $griz$ filter as functions of PT color (see Figure 3). Least-squares polynomial fits to the data provide quantitative offsets between the $(griz)_{PT}$ and $(griz)_{SDSS}$ systems (see §3.2). Two-part piecewise functions were used for the g_{PT} and r_{PT} corrections which were functions of $(r-i)_{PT}$. These fits both had breaks at $(r-i)_{PT} = 1.25$ and were found to be better fits to the data than single polynomials.

Systematic selection of stars in the blue end of the data shown in Figure 3 occurs due to the color cuts chosen in the PT and SDSS sample selection. Our fitting regions, shown in Figure 3 and listed in Table 2, avoid these areas.

⁸ <http://cas.sdss.org/dr5/en/>

⁹ Specifically, we required detections in BINNED1 in the r , i and z bands. We also selected against r , i and z observations with the EDGE, NOPROFILE, PEAKCENTER, NOTCHECKED, PSF_FLUX_INTERP, SATURATED, DEBLEND_NOPEAK, INTERP_CENTER, COSMIC_RAY or BAD_COUNTS_ERROR flags set, as well as observations with psf magnitude errors greater than 0.2 mag.

¹⁰ <http://das.sdss.org/PT/>

To remove any strong outliers, (i.e. visual binaries, mismatches, and flares), our fits are weighted by photometric error and are based only on data with a photometric error less than 0.05 magnitudes in every color band for each observation.

3.2. Transformations

The following equations produce the fits shown in Figure 3. These fits provide the best transformation of $(griz)_{PT}$ data to the native $(griz)_{SDSS}$ system for red stars.

$$\begin{aligned} g_{SDSS}(0.6 \leq (r-i)_{PT} < 1.25) &= g_{PT} + 0.142 - 0.514(r-i)_{PT} + 0.647(r-i)_{PT}^2 \\ &\quad - 0.241(r-i)_{PT}^3 \pm 0.072, \\ g_{SDSS}(1.25 \leq (r-i)_{PT} \leq 1.7) &= g_{PT} - 2.511 + 5.391(r-i)_{PT} - 3.787(r-i)_{PT}^2 \\ &\quad + 0.885(r-i)_{PT}^3 \pm 0.082 \end{aligned} \quad (1)$$

$$\begin{aligned} r_{SDSS}(0.6 \leq (r-i)_{PT} < 1.25) &= r_{PT} + 0.116 - 0.339(r-i)_{PT} + 0.301(r-i)_{PT}^2 \\ &\quad - 0.091(r-i)_{PT}^3 \pm 0.043, \\ r_{SDSS}(1.25 \leq (r-i)_{PT} \leq 1.7) &= r_{PT} + 0.003 - 0.009(r-i)_{PT} \pm 0.055 \end{aligned} \quad (2)$$

$$\begin{aligned} i_{SDSS}(0.6 \leq (r-i)_{PT} \leq 1.7) &= i_{PT} - 0.019 + 0.082(r-i)_{PT} - 0.068(r-i)_{PT}^2 \\ &\quad + 0.024(r-i)_{PT}^3 \pm 0.033 \end{aligned} \quad (3)$$

$$\begin{aligned} z_{SDSS}(0.35 \leq (i-z) \leq 0.8) &= z_{PT} - 0.285 + 1.566(i-z)_{PT} - 2.637(i-z)_{PT}^2 \\ &\quad + 1.488(i-z)_{PT}^3 \pm 0.050 \end{aligned} \quad (4)$$

These equations are valid for the color ranges listed in Table 2, and should **only** be employed within these ranges. Also, these corrections are applicable only to PT observations which have been reduced by MTPIPE and not USNO $u'g'r'i'z'$ data. After applying the transformations, there is a significant improvement in the average colors of the stellar locus of red stars. As shown in Figure 4, the PT data from Figure 1 align with the SDSS stellar locus when the new transformations are employed. Although the corrections from Equations 1-4 are small, the offsets amount to more than 0.1 mag in $(g-r)$ for the reddest stars. Corrections in the $(r-i)$, $(i-z)$ diagram (Figure 5) are less substantial, but still significant.

4. DISCUSSION

We have matched a large sample of background red stars observed with the PT to photometric observations of the same stars in the SDSS DR5 catalog. We present transformations based on magnitude differences between the $(griz)_{PT}$ and $(griz)_{SDSS}$ photometric systems as functions of color.

These transformations provide a significant improvement in the photometric calibration of PT data onto the SDSS 2.5-m system for red stars. Our results augment the initial transformations described in T06 which have already been applied to all publicly available PT data. The systematic color offsets for red stars, corresponding to spectral types M0 through M5 (Bochanski et al. 2007a), which have previously been seen between the PT and SDSS (see Figures 4 and 5) are corrected when our transformations are applied.

The ability to place the $(griz)_{PT}$ photometry onto the native SDSS 2.5-m system allows PT observations to serve as a ‘bright extension’ of the SDSS survey. In particular, PT observations of red stars with measured trigonometric parallaxes can now be reliably transformed onto the SDSS 2.5m system with a typical accuracy $< 10\%$, allowing an improved definition of the color-magnitude relation for low-mass stars in native SDSS color-space (Hawley et al. 2002; West et al. 2005; Davenport et al. 2006). We expect these results to be useful in analyzing targeted PT observations of red dwarf parallax standards (Williams et al. 2002; Golimowski et al. 2007), as well as serendipitous PT observations of stars with Hipparcos parallaxes.

The authors would like to thank Douglas Tucker and David Golimowski for their insightful comments, suggestions, and assistance with MTPIPE. The authors acknowledge the support of NSF grants AST02-05875, AST06-07644, and NASA ADP grant NAG5-1211. K.R.C. acknowledges support for this work was provided by NASA through the Spitzer Space Telescope Fellowship Program, through a contract issued by the Jet Propulsion Laboratory, California Institute of Technology under a contract with NASA. A.A.W. acknowledges the support of NSF grant AST05-40567.

This project made extensive use of SDSS data. Funding for the SDSS and SDSS-II has been provided by the Alfred P. Sloan Foundation, the Participating Institutions, the National Science Foundation, the U.S. Department of Energy, the National Aeronautics and Space Administration, the Japanese Monbukagakusho, the Max Planck Society, and the Higher Education Funding Council for England. The SDSS Web Site is <http://www.sdss.org/>.

The SDSS is managed by the Astrophysical Research Consortium for the Participating Institutions. The Participating Institutions are the American Museum of Natural History, Astrophysical Institute Potsdam, University of Basel, Cambridge University, Case Western Reserve University, University of Chicago, Drexel University, Fermilab, the Institute for Advanced Study, the Japan Participation Group, Johns Hopkins University, the Joint Institute for Nuclear Astrophysics, the Kavli Institute for Particle Astrophysics and Cosmology, the Korean Scientist Group, the Chinese Academy of Sciences (LAMOST), Los Alamos National Laboratory, the Max-Planck-Institute for Astronomy (MPIA), the Max-Planck-Institute for Astrophysics (MPA), New Mexico State University, Ohio State University, University of Pittsburgh, University of Portsmouth, Princeton University, the United States Naval Observatory, and the University of Washington.

We finally would like to thank the anonymous referee for their helpful comments and questions.

REFERENCES

- Adelman-McCarthy, J., et al. 2007, ApJS submitted
 Bochanski, J. J., West, A. A., Hawley, S. L., & Covey, K. R. 2007a, AJ, 133, 531
 Bochanski, J. J., et al. 2007b, AJ, submitted
 Chiu, K., Fan, X., Leggett, S. K., Golimowski, D. A., Zheng, W., Geballe, T. R., Schneider, D. P., & Brinkmann, J. 2006, AJ, 131, 2722
 Covey, K. C., et al. 2007, in preparation
 Davenport, J. R. A., West, A. A., Matthiesen, C. K., Schmieding, M., & Kobelski, A. 2006, PASP, 118, 1679
 Fan, X. 1999, AJ, 117, 2528
 Fukugita, M., Ichikawa, T., Gunn, J. E., Doi, M., Shimasaku, K., & Schneider, D. P. 1996, AJ, 111, 1748
 Golimowski, D. A., et al. 2007, in preparation
 Gunn, J. E. et al. 1998, AJ, 116, 3040
 —. 2006, AJ, 131, 2332
 Hawley, S. L. et al. 2002, AJ, 123, 3409
 Hogg, D. W., Finkbeiner, D. P., Schlegel, D. J., & Gunn, J. E. 2001, AJ, 122, 2129
 Ivezić, Ž. et al. 2004, Astronomische Nachrichten, 325, 583
 Metchev, S. A., et al. 2007, in preparation
 Pier, J. R., Munn, J. A., Hindsley, R. B., Hennessy, G. S., Kent, S. M., Lupton, R. H., & Ivezić, Ž. 2003, AJ, 125, 1559
 Skrutskie, M. F. et al. 1997, in ASSL Vol. 210: The Impact of Large Scale Near-IR Sky Surveys, ed. F. Garzon, N. Epchtein, A. Omont, B. Burton, & P. Persi, 25
 Smith, J. A. et al. 2002, AJ, 123, 2121
 Stoughton, C. et al. 2002, AJ, 123, 485
 Strauss, M. A. et al. 1999, ApJ, 522, L61
 Tucker, D. L. et al. 2006, Astronomische Nachrichten, 327, 821
 Walkowicz, L. M., Hawley, S. L., & West, A. A. 2004, PASP, 116, 1105
 West, A. A., Bochanski, J. J., Hawley, S. L., Cruz, K. L., Covey, K. R., Silvestri, N. M., Reid, I. N., & Liebert, J. 2006, AJ, 132, 2507
 West, A. A. et al. 2004, AJ, 128, 426
 West, A. A., Walkowicz, L. M., & Hawley, S. L. 2005, PASP, 117, 706
 West, A. A., et al. 2007, in preparation
 Williams, C. C. et al. 2002, BAAS, 34, 1292.
 York, D. G. et al. 2000, AJ, 120, 1579

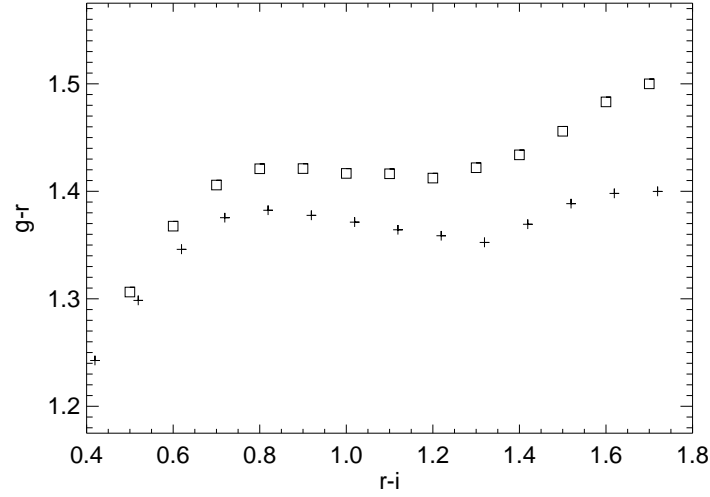


FIG. 1.— Median $(g-r)$, $(r-i)$ colors of low-mass stars. The SDSS data shown as open squares are on the $(ugriz)_{SDSS}$ system, PT data (crosses) are on the $(ugriz)_{PT}$ system. Note the ~ 0.1 magnitude offset between the two stellar loci for red $(r-i)$ colors.

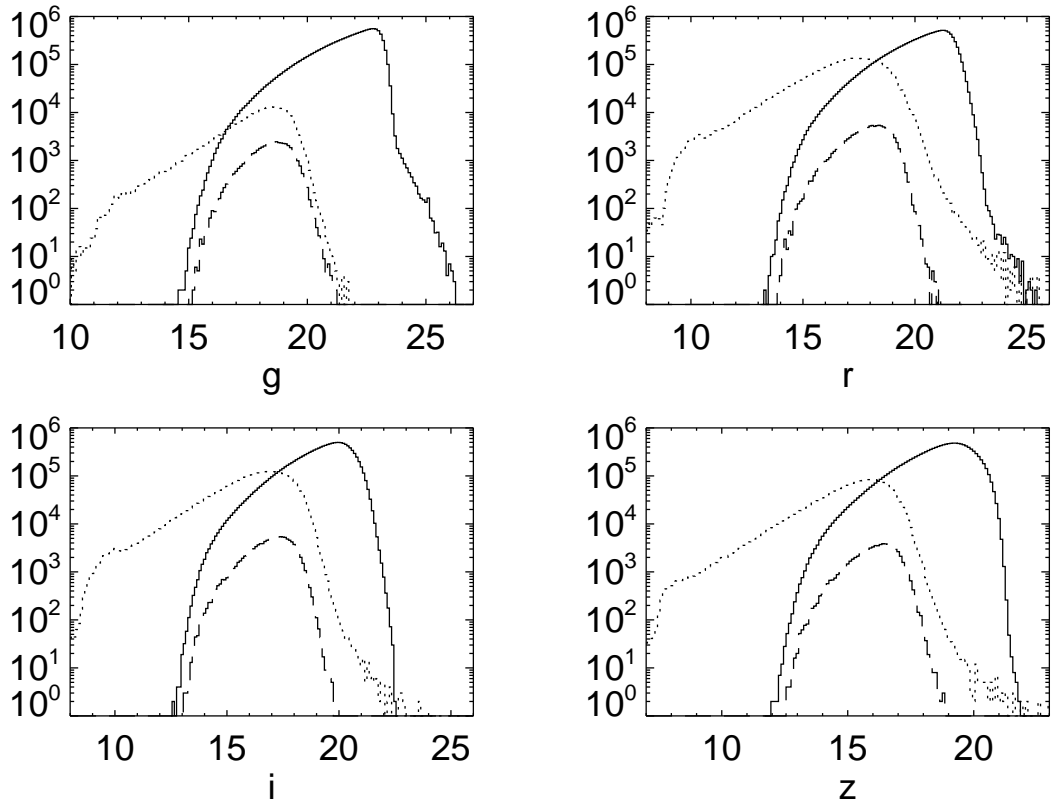


FIG. 2.— Histograms of the full five million PT (dotted line) and 13.6 million SDSS (solid line) data sets. Note the brighter limits of the smaller PT telescope. The matched sub-sample of $\sim 43,000$ stars is shown as the dashed line for each filter.

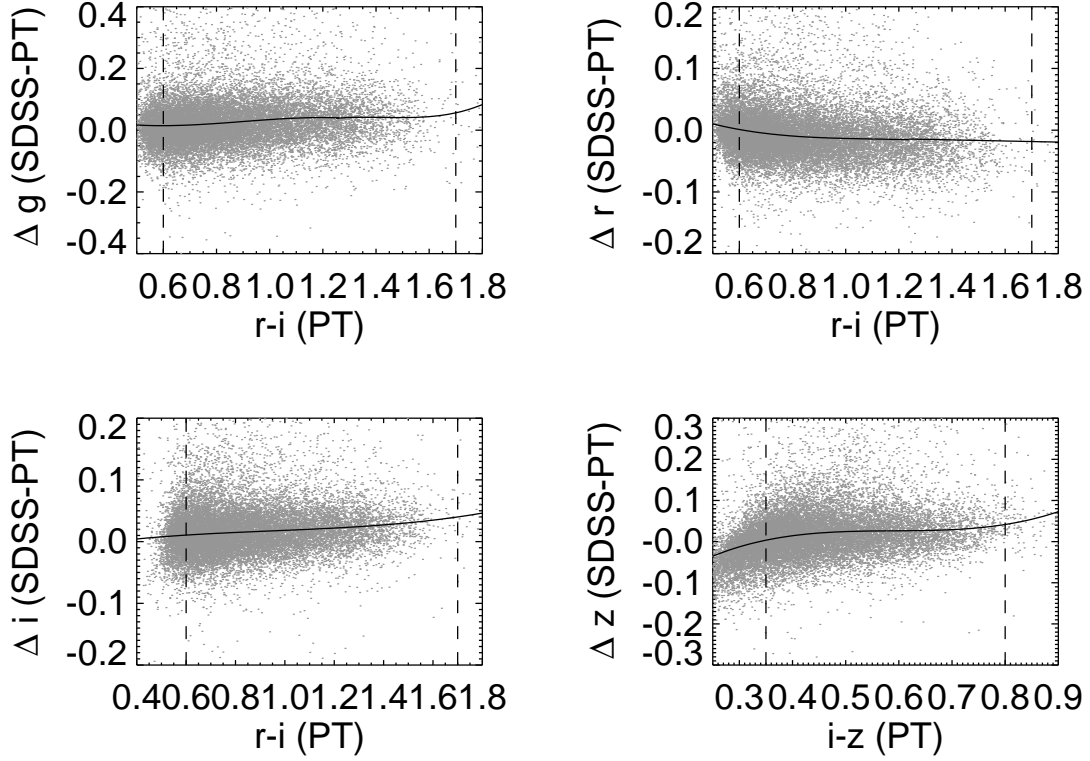


FIG. 3.— Difference in PT and SDSS magnitudes as a function of $(r-i)_{PT}$ and $(i-z)_{PT}$ color. Error weighted polynomial least-squares fits are shown as solid lines in each panel. The vertical dashed lines indicate the color ranges over which the fits are reliable.

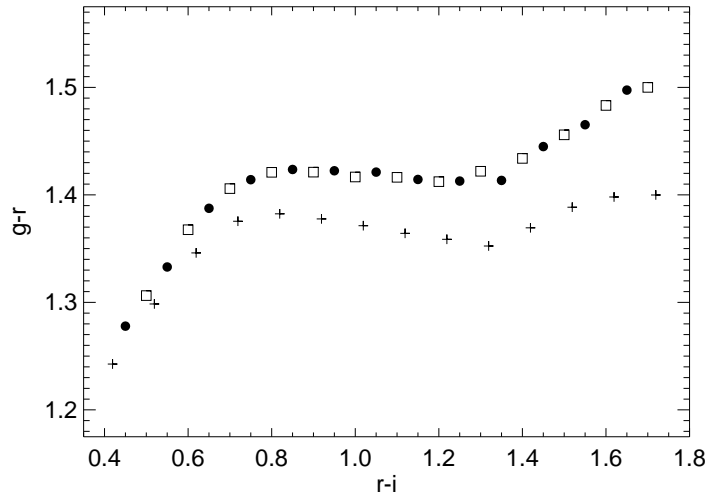


FIG. 4.— Median $(g-r)$, $(r-i)$ colors of low-mass stars as in Figure 1. gr_{iSDSS} data are shown as open squares. gr_{iPT} data prior to our corrections are shown as crosses, while gr_{iPT} data transformed using the equations in §3.2 are shown as filled circles.

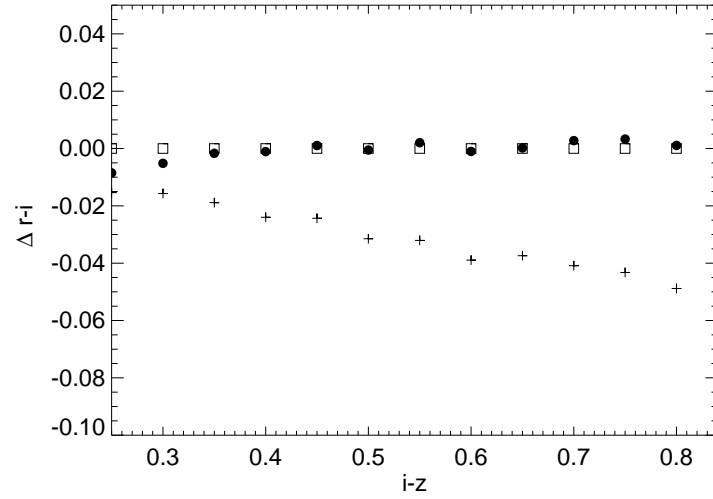


FIG. 5.— Median $\Delta(r-i)$, $(i-z)$ residuals of low-mass stars. SDSS - SDSS data are shown as open squares. SDSS - PT data on the SDSS system prior to our corrections are shown as crosses, while SDSS - PT data transformed using the equations in §3.2 are shown as filled circles.

TABLE 1
TUCKER ET AL. (2006) PT
STANDARD STAR COLOR
RANGES

Color
$0.70 \leq (u - g)_{PT} \leq 2.70$
$0.15 \leq (g - r)_{PT} \leq 1.20$
$-0.10 \leq (r - i)_{PT} \leq 0.60$
$-0.20 \leq (i - z)_{PT} \leq 0.40$

TABLE 2
APPLICABLE COLOR
RANGES FOR EQUATIONS
1-4

Color
$1.20 \leq (g - r)_{PT} \leq 1.55$
$0.60 \leq (r - i)_{PT} \leq 1.70$
$0.35 \leq (i - z)_{PT} \leq 0.80$